http://www.jstage.jst.go.jp/browse/biophysics

BIOPHYSICS

Vol. 7, pp. 59–67 (2011)
doi: 10.2142/biophysics.7.59

# Characterization of the flagellar motor composed of functional GFP-fusion derivatives of FliG in the $Na^+$-driven polar flagellum of *Vibrio alginolyticus*

Masafumi Koike[1], Noriko Nishioka[1], Seiji Kojima[1] and Michio Homma[1]

[1]*Division of Biological Science, Graduate School of Science, Nagoya University, Chikusa-Ku, Nagoya 464-8602, Japan*

Received 19 July, 2011; accepted 18 August, 2011

**The polar flagellum of *Vibrio alginolyticus* is driven by sodium ion flux via a stator complex, composed of PomA and PomB, across the cell membrane. The interaction between PomA and the rotor component FliG is believed to generate torque required for flagellar rotation. Previous research reported that a GFP-fused FliG retained function in the *Vibrio* flagellar motor. In this study, we found that N-terminal or C-terminal fusion of GFP has different effects on both torque generation and the switching frequency of the direction of flagellar motor rotation. We could detect the GFP-fused FliG in the basal-body (rotor) fraction although its association with the basal body was less stable than that of intact FliG. Furthermore, the fusion of GFP to the C-terminus of FliG, which is believed to be directly involved in torque generation, resulted in very slow motility and prohibited the directional change of motor rotation. On the other hand, the fusion of GFP to the N-terminus of FliG conferred almost the same swimming speed as intact FliG. These results are consistent with the premise that the C-terminal domain of FliG is directly involved in torque generation and the GFP fusions are useful to analyze the functions of various domains of FliG.**

**Key words:** *Vibrio alginolyticus*, flagellar motor, $Na^+$-driven, basal body, FliG, GFP, C-ring

Abbreviations: CCW, counter-clockwise; CW, clockwise; CHAPS, 3-(3-cholamidepropyl) dimethylammonio-1-propanesulphonate.

Corresponding author: Michio Homma, Division of Biological Science, Graduate School of Science, Nagoya University, Chikusa-Ku, Nagoya 464-8602, Japan. e-mail: g44416a@cc.nagoya-u.ac.jp

The bacterial flagellar motor is a rotary nano-motor which converts the electrochemical potential difference of the coupling ion ($H^+$ or $Na^+$) into rotational energy. *Escherichia coli* and *Salmonella* have $H^+$-driven motors while *Vibrio alginolyticus* has a $Na^+$-driven motor. The rotation speed of the *Vibrio* motor is remarkably fast, 1,100 Hz on average and up to 1,700 Hz maximum, which is more than 4 times faster than the *E. coli* motor[1,2].

The flagellum is coordinately and hierarchically constructed of more than 30 related proteins and is composed of a rotor, stator, universal joint (hook) and helical filament[3,4]. The rotor part (also called the basal body) contains four rings and a drive shaft, which are named the L, P, MS and C rings and the rod, respectively[5,6]. The L, P, MS and C rings are thought to be located in positions corresponding to the outer membrane, the peptidoglycan layer, the cytoplasmic membrane and the cytoplasm, respectively[7]. The stator is responsible for torque generation. The stator unit is composed of MotA and MotB in *E. coli* or PomA and PomB in *Vibrio* spp., and is a hetero-hexamer of 4 A subunits and 2 B subunits[8-11]. Those subunits assemble around the rotor and conduct the coupling ions ($H^+$ in *E. coli* and $Na^+$ in *Vibrio*) due to their electrochemical potential across the cytoplasmic membrane[12,13]. In the $Na^+$-driven motor, additional motor proteins, MotX and MotY, are required for force generation[14,15].

Genetic evidence indicates that the C ring is composed of 3 different proteins, FliG, FliM and FliN and is essential for torque generation, switching the rotational direction, and flagellation[5,16,17]. FliG appears to be most directly involved in the torque generation[18]. Mutational analysis suggests that electrostatic interactions between conserved charged residues

in the C-terminal domain of FliG and the cytoplasmic domain of MotA are required for the torque generation[19] although this may not hold true for the $Na^+$-type motor of *V. alginolyticus*[20,21]. FliM interacts with the chemotactic signaling protein CheY in its phosphorylated form (CheY-P) to regulate rotational direction[22]. FliN mostly contributes to forming the C-ring structure along with FliM and it also interacts with CheY-P[23,24]. The spatial distribution of these proteins in the C ring of *Salmonella* has been visualized by electron microscopy and single particle image analysis[25]. However, the correct positioning of these 3 proteins has still not been clarified.

In the $Na^+$-driven motor of *V. alginolyticus*, a novel ring structure, called the T ring, was found in the purified basal-body structure of the polar flagellum[26]. The T ring is composed of MotX and MotY and is located below the LP ring[26,27]. It has been suggested that MotX interacts with MotY and PomB[28,29]. The T ring was proposed to be involved in the incorporation and/or stabilization of the PomA/B complex into the motor and to thus provide a connection between the basal body and PomA/B in *Vibrio*[26]. More recently, a novel H ring structure which forms the outer rim of the LP ring was found in the basal body of the $Na^+$-driven motor; the H ring is lost in the *flgT* mutant and the *flgT* gene or H ring is involved in motility as well as in flagellation[30].

Fluorescence microscopy of GFP-fused proteins is frequently used to investigate the subcellular localization of a protein of interest. *V. alginolyticus* has a polar flagellum at one side of its cell pole and therefore we can easily observe the localization of flagellar motor proteins at the flagellated cell pole[20,31]. In a previous study, we reported that GFP fusion at either the N or the C terminus of FliG is polar localized and still functional in the *Vibrio* flagellar motor, although swarming and swimming ability are decreased[20]. In a $H^+$-driven motor, either GFP-fusion severely impaired or destroyed its function[32–34]. However, the effects of GFP fusion on flagellar function have not been characterized well and it has not been directly shown that the GFP-fused FliG is assembled onto the cytoplasmic face of the MS ring of the flagellar rotor. In this study, we found that GFP-fused FliG worked more efficiently than we expected in the motor of *V. alginolyticus*. We compared the ability to confer motility by the N-terminally or C-terminally GFP-fused FliG and the structure of the isolated rotor with each GFP-fused FliG protein.

## Materials and Methods

### Bacterial strain, plasmids, growth conditions and media

The strains and plasmids used in this study are listed in Table 1. The mutation of Δ*fliG* was introduced into KK148 as described previously[20] and the resultant strain was named MK1. *V. alginolyticus* was cultured at 30°C in VC medium [0.5% (w/v) Polypepton, 0.5 % (w/v) yeast extract, 0.4% (w/v) $K_2HPO_4$, 3% (w/v) NaCl, 0.2% (w/v) glucose] or VPG medium [1% (w/v) Polypepton, 0.5% (w/v) glycerol, 0.4% (w/v) $K_2HPO_4$, 3% (w/v) NaCl]. Chloramphenicol was added to a final concentration of 2.5 μg/ml for *V. alginolyticus*.

**Table 1** Bacterial strains and plasmids

| Strain or plasmid | Genotype or description | Reference |
|---|---|---|
| *V. alginolyticus* strains | | |
| VIO5 | *laf* ($Rif^r$ $Pof^+$ $Laf^-$) | (15) |
| KK148 | *flhG* (multi-$Pof^+$) *laf* ($Rif^r$ $Pof^+$ $Laf^-$) | (35) |
| NMB198 | Δ*fliG laf* ($Rif^r$ $Pof^+$ $Laf^-$) | (20) |
| MK1 | Δ*fliG flhG* (multi-$Pof^+$) *laf* ($Rif^r$ $Pof^+$ $Laf^-$) | This work |
| *Plasmids* | | |
| pBAD33 | $P_{BAD}$ $Cm^r$ | (36) |
| pTY102 | *gfp* in pBAD33 | (20) |
| pTY200 | *fliG* in pBAD33 | (20) |
| pTY201 | *gfp-fliG* in pBAD33 | (20) |
| pTY202 | *fliG-gfp* in pBAD33 | (20) |

$Rif^r$, rifampicin resistant; $Pof^+$, normal polar flagellar formation; $Laf^-$, defective in lateral flagellar formation; $Mot^-$, non-motile; multi-$Pof^+$, multiple polar flagellar formation; $Cm^r$, chloramphenicol resistant; $P_{BAD}$, *araBAD* promoter.

### Swarming assay

VPG500 semisolid agar [1% (w/v) bactotryptone, 0.4% (w/v) $K_2HPO_4$, 500 mM NaCl, 0.5% (w/v) glycerol and 0.25% (w/v) bactoagar] was used for motility assays of *V. alginolyticus*. One μl aliquot of an overnight culture was spotted onto VPG500 semisolid agar and incubated at 30°C for the desired time.

### Measurement of swimming speed

Overnight cultures were inoculated into VPG500 medium containing 0.02% (w/v) arabinose and 2.5 μg/ml chloramphenicol at a 100-fold dilution. The cells were incubated at 30°C for 4 hr and were then collected by centrifugation at 2,000×g for 5 min. The cells were re-suspended in TMN500 buffer [50 mM Tris-HCl, pH 7.0, 5 mM $MgCl_2$, 5 mM glucose, 500 mM NaCl]. The suspensions were re-centrifuged and then resuspended using the TMN buffer, and cells were diluted 1/50 in the TMN buffer and kept at room temperature for 15 min. Swimming of the cells was observed using dark-field microscopy immediately after the addition of serine to a final concentration of 20 mM. Swimming speeds were determined for at least 20 individual cells. Images of cells were recorded on a video recorder, and their swimming speeds were measured using software for motion analysis (Move-tr/2D, Library Co., Tokyo, Japan).

### Immunoblotting

Samples were suspended in SDS loading buffer and boiled at 95°C for 5 min, and SDS-polyacrylamide gel electrophoresis (PAGE) and immunoblotting were performed as described previously[37]. Antisera against MotY (MotYB0079), FliG (FliGB0164), GFP (BD living colors), Flagellin (PF42), and PomA (PomA1312) were prepared as previously reported[37–40]. HRP (horse radish peroxidase)-linked

goat anti-rabbit IgG (Santa Cruz, Santa Cruz, CA) was used as the secondary antibody.

**Introduction of plasmids into *V. alginolyticus***

Transformations were carried out by electroporation as described previously[41].

**Isolation of the flagellar rotor**

We followed the published protocol for the isolation of flagellar rotors with intact FliG[38].

**Sucrose density gradient centrifugation**

The purified rotors were applied on top of a 20–60% (w/w) stepwise sucrose gradient in TEC [10 mM Tris-HCl, pH 8.0, 5 mM EDTA, 0.5% (w/v) CHAPS]. After centrifugation at 72,000×*g* for 90 min at 4°C, the gradient was divided into 20 fractions from the top to the bottom[38].

**Fluorescent microscopy**

To observe the subcellular localization of GFP-fused FliG by fluorescent microscopy, MK1 cells harboring a plasmid were cultured overnight in VC medium, then diluted 100-fold in VPG medium containing 2.5 μg/ml chloramphenicol and 0.1% arabinose. Cells were cultured for 4 hr at 30°C, harvested and suspended into TMN500 medium [50 mM Tris-HCl, pH 7.5, 5 mM $MgCl_2$, 5 mM glucose, 500 mM NaCl]. Suspended cells were fixed by 0.1% (w/v) poly-L-lysine, and observed by fluorescence microscopy (Olympus, BX50, Japan) as described previously[31]. The images were captured by a digital camera (Hamamatsu Photonics, C4742-80-12AG, Japan) and processed using imaging software (Scanalytics, IP lab, version 3.9.5r2).

**Electron microscopy**

*Vibrio* cells or samples containing flagellar structures were put on hydrophilic-treated carbon coated copper grids. The grids were washed with buffer [10 mM Tris-HCl, pH 8.0, 5 mM EDTA], negatively stained with 2% potassium phosphotungstate or 3% uranyl acetate and observed with a JEM-1200EX or JEM-2010 electron microscope (JEOL, Tokyo, Japan).

## Results

**Detection of GFP-fused FliG proteins**

To analyze GFP-fused FliG proteins (N terminal and C terminal FliG are termed GFP-FliG and FliG-GFP, respectively), we used the multiple polar flagellar *V. alginolyticus* strain, KK148, which is a *flhG* mutant that expresses the flagellar genes at levels higher than wild-type[34]. GFP-FliG and FliG-GFP were produced from plasmid vectors using arabinose as an inducer in a *fliG* deleted strain (MK1, hereafter described as the *fliG flhG* strain) which was constructed from KK148. The GFP-fused FliG proteins in the *Vibrio* cells were detected by western blotting using anti-FliG and anti-GFP antibodies (Fig. 1). The molecular weights of GFP and FliG are 27 kDa and 39 kDa, respectively, and thus the fusion protein is estimated as 66 kDa. From whole cell lysates, the 62 kDa band was strongly detected by the anti-FliG antibody and corresponded to the size of the fusion protein (Fig. 1a and 1b). Several bands smaller than 62 kDa were detected in GFP-FliG as well as FliG-GFP. Those smaller bands might represent degradation or truncated products of the fusion proteins, suggesting that there are some differences in stability between GFP-FliG and FliG-GFP, and that the stability of GFP-FliG is relatively

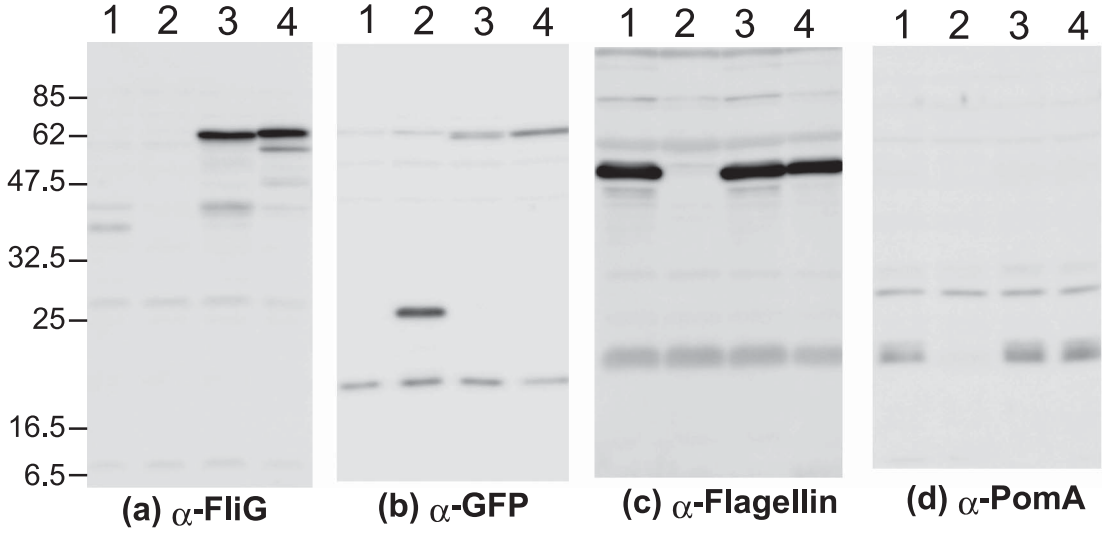


**Figure 1** Protein expression profiles. MK1 cells harboring plasmids (1: pTY102 (FliG), 2: pTY200 (GFP), 3: pTY202 (FliG-GFP), or 4: pTY201 (GFP-FliG)) were grown at 30°C for 4 hr in VPG medium containing 2.5 μg/ml chloramphenicol and 0.1% arabinose. Whole cell extracts were subjected to SDS-PAGE, followed by immunoblotting using anti-FliG (a), anti-GFP (b), anti-flagellin (c), and anti-PomA (d) antibodies.

lower than FliG-GFP. No effect on flagellar protein expression was detected by western blotting using anti-flagellin or anti-PomA antibodies (Fig. 1c and 1d). The expressions of flagellin and the motor protein, PomA, were repressed by the *fliG* mutation according to the transcriptional hierarchy of the flagellar regulon.

**Function of GFP-fused FliG in the *Vibrio* flagellar motor**

Either GFP-fused FliG could confer the swarming ability to the *fliG* mutant as well as the *fliG flhG* mutant in soft-agar VPG plates although their swarming size was much smaller than the wild-type FliG (Fig. 2). The swarming ability of GFP-FliG was slightly higher than that of FliG-GFP, indicating that the effect of GFP fusion on the motor function of FliG is different depending on whether the GFP is fused to the N or the C terminal region.

The subcellular localizations of GFP-fused FliG proteins were observed by fluorescent microscopy in *fliG flhG* cells.

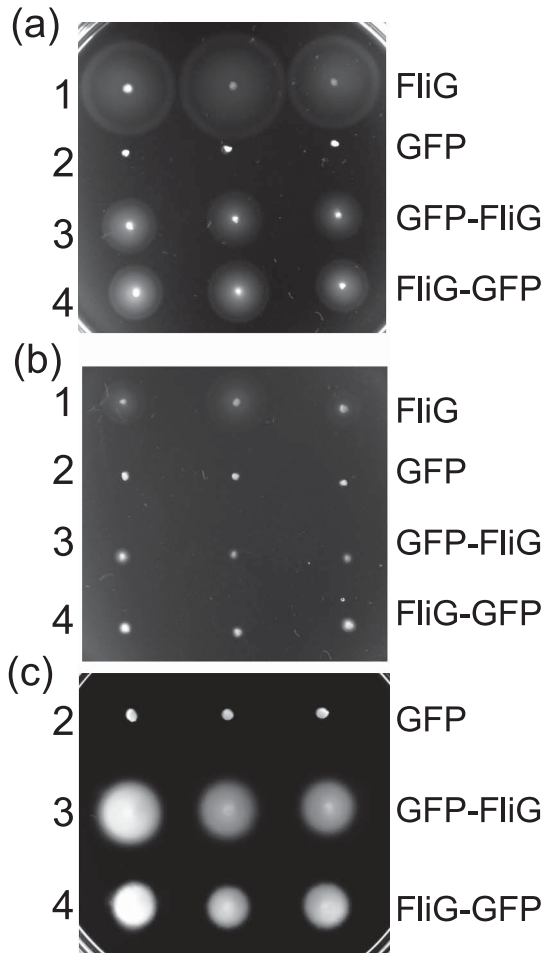


**Figure 2** Swarming abilities of multiple polar flagella mutants. Fresh colonies of NMB198 (a) or MK1 (b and c) cells harboring plasmids (1: pTY102 (FliG), 2: pTY200 (GFP), 3: pTY201 (GFP-FliG), or 4: pTY202 (FliG-GFP)) were inoculated on 0.25% agar VPG plates containing 2.5 μg/ml chloramphenicol and 0.1% arabinose, and were then incubated at 30°C for 6 hr (a and b) or 24 hr (c).

GFP was distributed throughout the cells and was not localized at the cell poles. Intense fluorescent dots of both GFP-fused FliG were detected at cell poles as reported previously (Fig. 3). However, the intensity of those dots was much stronger than the fluorescent dots of *fliG* cells without the *flhG* mutation. We could not observe the difference of the fluorescent dot profiles between GFP-FliG and FliG-GFP.

Next, flagellated *Vibrio* cells expressing GFP-fused FliG were observed using negative staining and electron microscopy. Profiles of the flagellation were not different between wild-type FliG cells and GFP-fused FliG cells (Fig. 4). These results show that the GFP fusion does not affect the flagellar morphogenesis at all.

**Swimming and chemotactic behavior of *Vibrio* expressing GFP-fused FliG**

To analyze in more detail the cell motility and behavior with GFP-fused FliG, swimming cells were observed by dark field microscopy. Although the effect of GFP fusion on swarming ability was severe (Fig. 2), the effect of GFP fusion on free swimming in buffer was not as severe as expected. GFP-FliG conferred almost the same swimming speed as wild-type FliG (wild-type FliG, 45±9.6 μm/sec; GFP-FliG, 41±9.3 μm/sec) and the chemotactic behavior or the switching frequency of the swimming direction seemed to be decreased. On the other hand, FliG-GFP conferred a slow swimming speed (9±3.8 μm/sec) and the swimming direction was not changed. When phenol was added to the buffer as a repellent, the switching of swimming cells expressing FliG-GFP was not changed although swimming cells expressing wild-type FliG switched in response to the repellent (data not shown). From these results, we conclude that GFP fused to FliG affects the torque generation and rotational switching of the motor differently depending on the fusion site.

**Isolation of the rotor with GFP-fused FliG**

The GFP-fused FliG is assembled into the flagellar motor and is functional. We wanted to see the GFP-fused proteins directly by electron microscopy in the flagellar rotors. Rotors (basal bodies) with GFP-fused FliG were isolated using a protocol developed to isolate the basal bodies of *V. alginolyticus* with FliG[38]. The basal bodies with GFP-FliG or FliG-GFP were isolated and fractionated by sucrose density gradient centrifugation. MotY and GFP-fused FliG were detected by western blotting (Fig. 5). The band peaks of both GFP-fused FliG proteins copurified with MotY, which is a marker protein of the basal body. We confirmed that the GFP-fused FliG proteins are associated with the basal body similar to wild-type FliG, as previously reported[38]. FliG was also detected in the upper fractions of the gradient (1 to 5), indicating that FliG is easily dissociated from the basal body. More FliG was detected in the upper fractions of the gradient from the GFP fused FliG than from the intact FliG. As for FliG-GFP, the degradation bands were detected in the

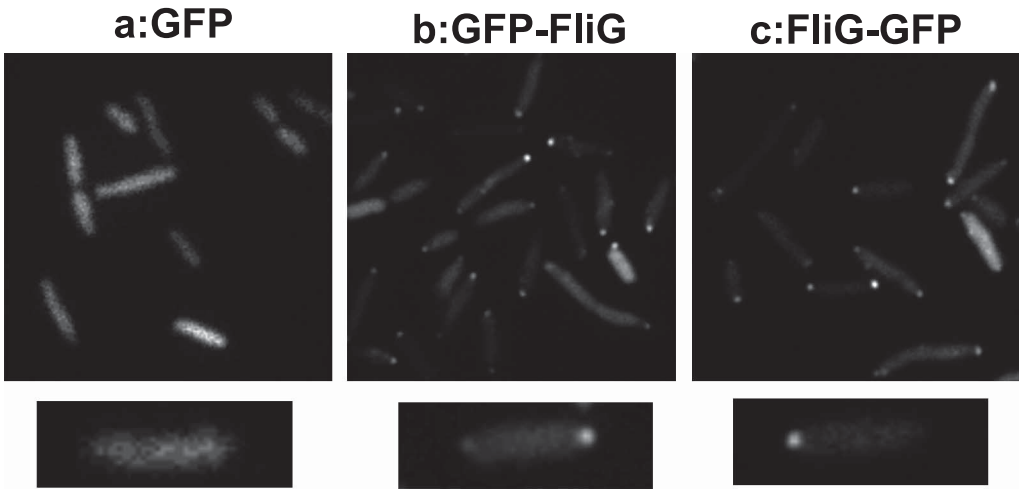


**Figure 3** Cellular localization of GFP-fused FliG in multiple polar flagella mutants. MK1 cells harboring plasmids (a: pTY200 (GFP), b: pTY201 (GFP-FliG), or c: pTY202 (FliG-GFP) ) were grown in VPG medium containing 2.5 μg/ml chloramphenicol and 0.1% arabinose at 30°C for 4 hr. Cells were observed by fluorescence microscopy as described in the Materials and Methods.

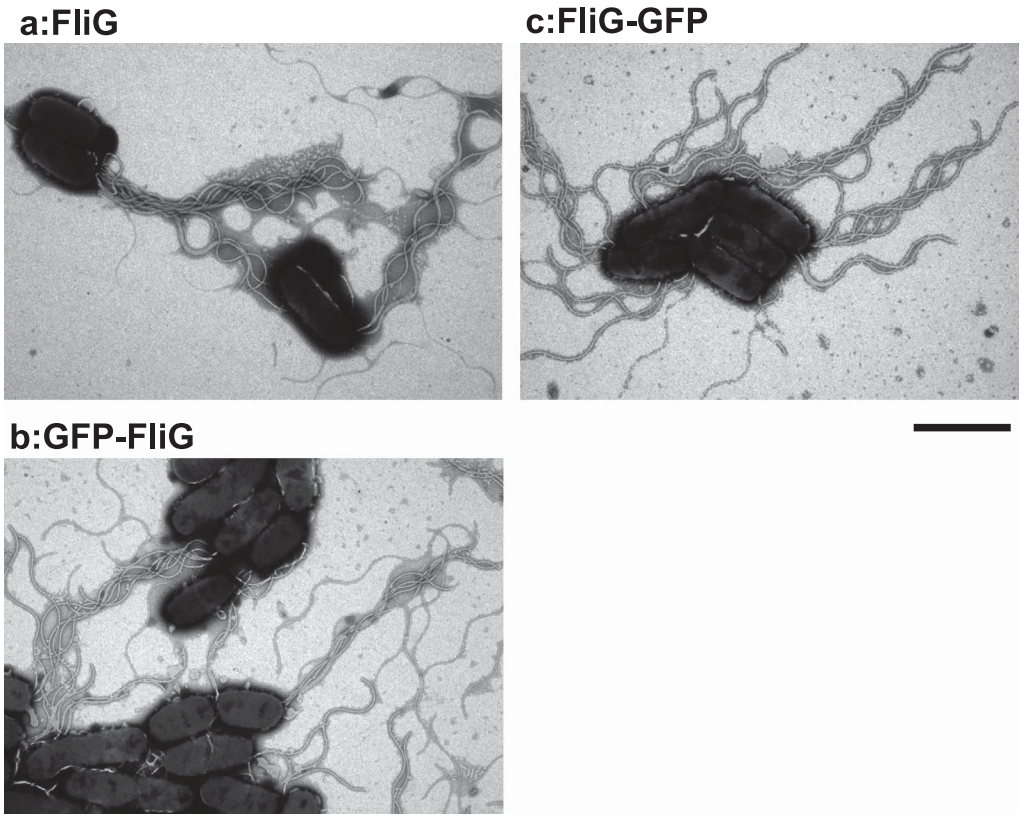


**Figure 4** Electron micrographs of flagella. MK1 cells harboring plasmids (a: pTY102 (FliG), b: pTY201 (GFP-FliG), or c: pTY202 (FliG-GFP) were grown in VC medium overnight and were inoculated into VPG medium containing 2.5 μg/ml chloramphenicol and 0.1% arabinose, and were then incubated at 30°C for 4 hr. Cells were harvested by centrifugation and were negatively stained with potassium phosphotungstate. Bar, 2 μm.

upper fractions. The basal bodies from peak fractions of FliG were observed by electron microscopy with negative staining. However, no structural difference due to the fused GFP was observed (data not shown). We may have to find a milder condition to purify the basal body or to make a stable construct of the fusion, such as the linker sequence is optimized.

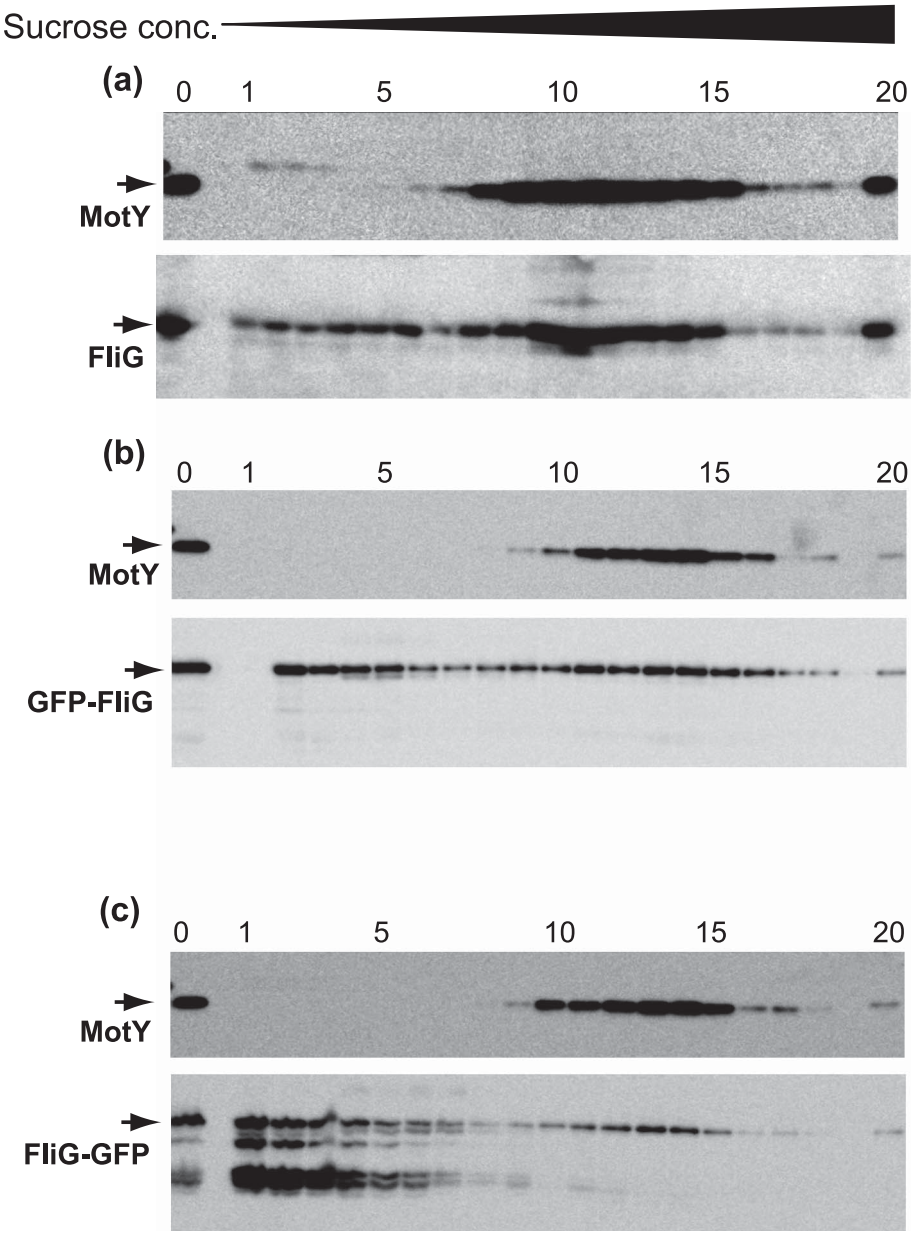


**Figure 5** Fractionation by sucrose density gradient centrifugation. The basal bodies were prepared from MK1 cells harboring plasmids pTY102 (FliG) (a), pTY201(GFP-FliG) (b), or pTY202 (FliG-GFP)(c). The basal bodies (lane 0) were applied to a 20–60% (w/w) stepwise sucrose gradient in TEC. After centrifugation at 72,000×g for 90 min at 4°C, the gradient was divided into 20 fractions from the top to the bottom. Proteins in each fraction were separated by SDS-PAGE and were detected by immunoblotting using anti-MotY (upper panel) or anti-FliG antibodies (lower panel).

## Discussion

A previous study by Yorimitsu *et al*. showed that the GFP-fused FliG at either the N terminus or the C terminus retained the function of FliG in the $Na^+$-driven motor of *V. alginolyticus*[20]. That was somewhat surprising because it is hard to imagine that the main motor protein required for energy conversion, which has a molecular weight of 39 kDa, is almost fully functional after the 27 kDa GFP is fused with it, and that the GFP fusion protein can still assemble into a ring structure as a part of the C ring. Similar fusions from *E. coli* had little or no function[32–34]. In a previous study, a strain with a point mutation in *fliG* was used. The site of the mutation was located at the codon for Arg135 (CGA) and was altered to the opal codon (TGA). In those cells, both types of GFP-fused FliG localized at the flagellar cell poles and were functional in flagellar rotation although the size of swarm ring was much smaller than the wild-type FliG. At that time, the report did not discuss what was the effect of the fused GFP on flagellar rotation and did

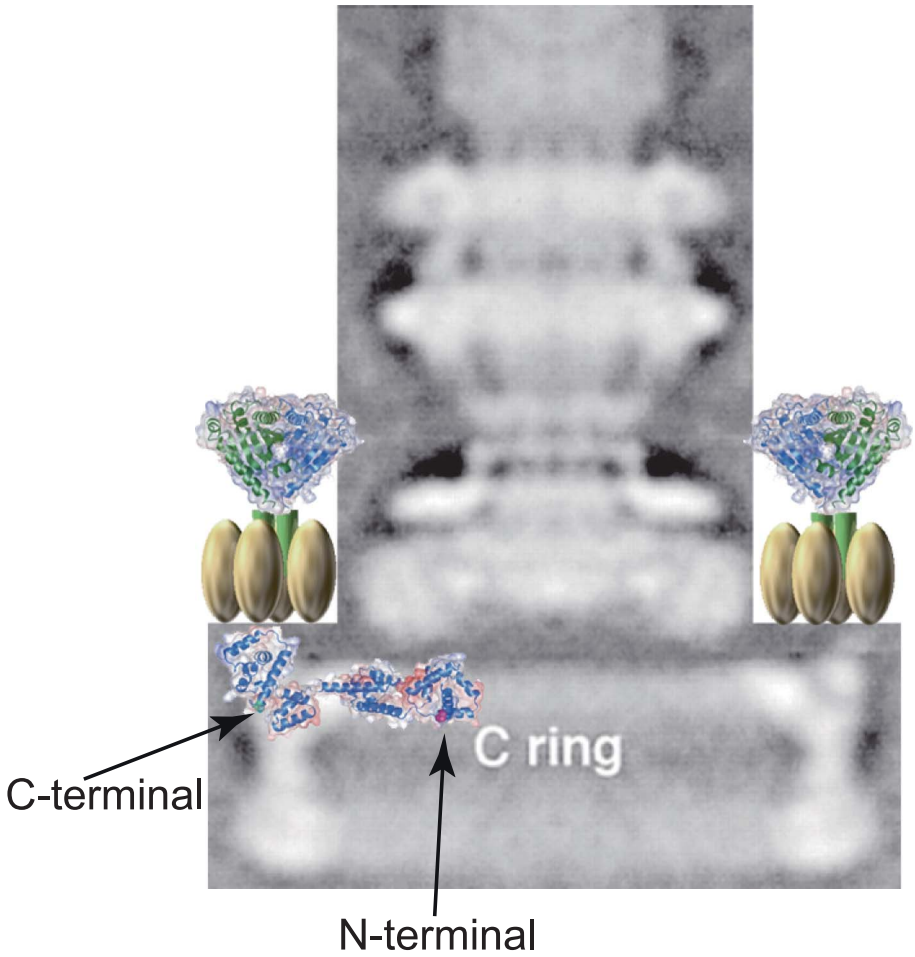


**Figure 6** Schematic location of GFP and FliG in the basal body. The stator complex and FliG are superimposed onto EM micrographs of the *S. typhimurium* flagellar basal body reported previously[5]. The structural model of intact FliG and C-terminal MotB was drawn by a pdb viewer of MolFeat (FiatLux Co., Tokyo, Japan) using pdb data of 3HJL and 2ZVZ, respectively.

not show that the GFP-fused FliG was assembled into the C ring. In this study, we constructed a *fliG* deleted mutant from the KK148 strain, which has the *flhG* mutation and has multiple polar flagella[35]. It should be much easier to analyze the function and structure of GFP-fused FliG in the flagellar motor because the number of rotors is 5 or 10 times more than the wild-type which has only a single flagellum in each cell.

GFP-FliG (N terminal fusion) retained the function for swimming and switching and that phenotype was similar to the wild-type FliG except for the decrease in swarming ability. The N terminal helices of FliG are believed to interact with FliF (MS ring), thus the fused GFP is expected to be located in the inside of the C ring, and therefore the bulky effect of GFP on flagellar function might be very small (Fig. 6). On the other hand, FliG-GFP (C terminal fusion) also worked in the flagellar motor, and both the swimming speed and the switching frequency were significantly reduced. Phenol, which is a repellent and induces a tumbling movement, did not work for the FliG-GFP motor. The swarming ability of FliG-GFP is comparable to that of GFP-FliG which conferd the better ability of swimming and switching. We do not know this reason and the slow motility may escape from the trap of cells by agar matrix. The C terminal region of FliG is believed to interact with a cytoplasmic domain of a stator protein and the interaction between conserved charged residues of FliG and the stator protein of MotA is essential to generate torque according to studies of *E. coli*[19]. However, these conserved residues are not essential for the *Vibrio* flagellar motor[20,21], and the C terminal regions in the species are exchangeable[20]. The C-terminal GFP is predicted to be present around the outer region of the C ring from a docking image of the crystal structure of FliG into the 3D EM reconstruction (Fig. 6)[25,42].

This C-terminal region plays an essential role in the torque generation and in the change of rotational direction, counter-clockwise (CCW) to clockwise (CW). This is probably consistent with the result that the fused GFP of the C-terminal region affects severely the motility as well as the chemotactic behavior. The switching of flagellar rotation for

chemotactic behavior is performed by CheY, the signal molecule for chemotaxis, which is phosphorylated and captured by the N terminal region of CheY, followed by interaction with FliM and FliN[23]. These interactions may cause some structural change(s) of FliG and switch the rotational direction from CCW to CW. The crystal structure of full length FliG ($FliG_{FL}$) was solved from *Aquifex aeolicus*[42], and the C terminal and middle domain of FliG ($FliG_{CM}$) was solved from *Thermotoga maritima*[43]. Although both structures are quite similar, there is an important difference in that the structure of the middle domain of $FliG_{FL}$ is the "open form" between $helix_{MC}$ and a single armadillo repeat motif ($ARM_M$), while $FliG_{CM}$ is the "closed form". All known FliG mutations that bias the direction of rotation of the flagellar motor have been mapped onto $FliG_{FL}$. Both CCW- and CW-biased mutations are located around $helix_{MC}$, and the CW-bias mutants occur at the $helix_{MC}$-middle domain interface. It was suggested that the solved "open" $FliG_{FL}$ is the CW state and the "closed" $FliG_{CM}$ is the CCW state for flagellar rotation. The different model for the structures of CCW and CW state was proposed from the crystal structure of the mutant $FliG_{MC}$ (ΔPEV) of *T. maritima*[44]. This mutant is corresponding to the CW-biased FliG mutant (ΔPAA) of *Salmonella*. When the structures were compared with the wild-type $FliG_{MC}$ which is CCW-biased, the conformational difference was found in helix E which connects $FliG_C$ and $FliG_M$. Helix E seems to be highly flexible and directly involved in the switching of the flagellar motor and it was proposed that a hinge motion of helix E may directly change the orientation of the neighboring $FliG_M$ domain to change the CCW or CW state[44]. The fused GFP of FliG in this study might inhibit the structural transitions between these two forms of FliG. When we purified the basal body associated with FliG-GFP by density gradient centrifugation, the amount of FliG-GFP associated with the basal body was much less than those of FliG and GFP-FliG. This is likely that the fused GFP at the C terminus disturbs the interaction between FliG and MS ring or between FliG by itself for the stable association in the basal body.

In *Salmonella*, structural analyses of the flagellar basal body have been done extensively, and the entire C-ring structure, including FliG, was solved by cryo-electron microscopy and single particle analysis[25]. In *Vibrio*, only FliG was isolated with the basal body. By electron microscopy, the location of FliG was not assigned in the image, thus it is speculated that FliG is too flexible even in the structure to observe it[45]. This flexibility might be an important property for the motor function to generate torque, for the directional change, or for connecting the MS-ring and the C-ring over symmetry mismatch[46,47]. In this study, the location of FliG was speculated from the density of the fused GFP on the basal body. A domain detection study using a GFP-tagged protein was reported from cytoplasmic dynein[48]. In electron microscopic observations of isolated rotors with GFP-fused FliG, structural differences were not detected. That may be due to FliG flexibility, and FliG cannot make a tight structure. It may also affect the difficulty in observing structures by electron microscopy. Alternatively, GFP-FliG may partially easily dissociate from the basal body during the isolation, and the number of associated FliG molecules on the MS ring may be not sufficient to observe.

## Acknowledgements

We thank T. Gotoh for technical advice about the electron microscopy and T. Terauchi for assistance in measuring the swimming speeds of cells.

This work was supported in part by grants-in-aid for scientific research from the Ministry of Education, Science, and Culture of Japan; and from the Japan Science and Technology Corporation (to M. H. and to S. K.).

## References

1. Kudo, S., Magariyama, Y. & Aizawa, S. Abrupt changes in flagellar rotation observed by laser dark-field microscopy. *Nature* **346**, 677–680 (1990).
2. Magariyama, Y., Sugiyama, S., Muramoto, K., Maekawa, Y., Kawagishi, I., Imae, Y. & Kudo, S. Very fast flagellar rotation. *Nature* **371**,752 (1994).
3. Hirano, T., Yamaguchi, S., Oosawa, K. & Aizawa, S. Roles of FliK and FlhB in determination of flagellar hook length in *Salmonella typhimurium*. *J. Bacteriol.* **176**, 5439–5449 (1994).
4. Samatey, F. A., Matsunami, H., Imada, K., Nagashima, S., Shaikh, T. R., Thomas, D. R., Chen, J. Z., Derosier, D. J., Kitao, A. & Namba, K. Structure of the bacterial flagellar hook and implication for the molecular universal joint mechanism. *Nature* **431**, 1062–1068 (2004).
5. Francis, N. R., Sosinsky, G. E., Thomas, D. & DeRosier, D. J. Isolation, characterization and structure of bacterial flagellar motors containing the switch complex. *J. Mol. Biol.* **235**, 1261–1270 (1994).
6. Ueno, T., Oosawa, K. & Aizawa, S. M ring, S ring and proximal rod of the flagellar basal body of *Salmonella typhimurium* are composed of subunits of a single protein, FliF. *J. Mol. Biol.* **227**, 672–677 (1992).
7. Aizawa, S. I. & Kubori, T. Bacterial flagellation and cell division. *Genes Cells* **3**, 625–634 (1998).
8. Braun, T. F., Al-Mawsawi, L. Q., Kojima, S. & Blair, D. F. Arrangement of core membrane segments in the MotA/MotB proton-channel complex of *Escherichia coli*. *Biochemistry* **43**, 35–45 (2004).
9. Kojima, S. & Blair, D. F. Solubilization and purification of the MotA/MotB complex of *Escherichia coli*. *Biochemistry* **43**, 26–34 (2004) .
10. Sato, K. & Homma, M. Functional reconstitution of the $Na^+$-driven polar flagellar motor component of *Vibrio alginolyticus*. *J. Biol. Chem.* **275**, 5718–5722 (2000).
11. Yorimitsu, T., Kojima, M., Yakushi, T. & Homma, M. Multimeric structure of the PomA/PomB channel complex in the $Na^+$-driven flagellar motor of *Vibrio alginolyticus*. *J. Biochem.* **135**, 43–51 (2004).
12. Kojima, S. & Blair, D. F. The bacterial flagellar motor: structure and function of a complex molecular machine. *Int. Rev. Cytol.* **233**, 93–134 (2004).
13. Yorimitsu, T. & Homma, M. $Na^+$-driven flagellar motor of *Vibrio*. *Biochim. Biophys. Acta.* **1505**, 82–93 (2001).
14. Okabe, M., Yakushi, T., Asai, Y. & Homma, M. Cloning and

characterization of *motX*, a *Vibrio alginolyticus* sodium-driven flagellar motor gene. *J. Biochem.* **130**, 879–884 (2001).
15. Okunishi, I., Kawagishi, I. & Homma, M. Cloning and characterization of *motY*, a gene coding for a component of the sodium-driven flagellar motor in *Vibrio alginolyticus*. *J. Bacteriol.* **178**, 2409–2415 (1996).
16. Yamaguchi, S., Aizawa, S., Kihara, M., Isomura, M., Jones, C. J. & Macnab, R. M. Genetic evidence for a switching and energy-transducing complex in the flagellar motor of *Salmonella typhimurium*. *J. Bacteriol.* **168**, 1172–1179 (1986).
17. Yamaguchi, S., Fujita, H., Ishihara, A., Aizawa, S. & Macnab, R. M. Subdivision of flagellar genes of *Salmonella typhimurium* into regions responsible for assembly, rotation, and switching. *J. Bacteriol.* **166**, 187–193 (1986).
18. Lloyd, S. A., Tang, H., Wang, X., Billings, S. & Blair, D. F. Torque generation in the flagellar motor of *Escherichia coli*: evidence of a direct role for FliG but not for FliM or FliN. *J. Bacteriol.* **178**, 223–231 (1996).
19. Zhou, J., Lloyd, S. A. & Blair, D. F. Electrostatic interactions between rotor and stator in the bacterial flagellar motor. *Proc. Natl Acad. Sci. U.S.A.* **95**, 6436–6441 (1998).
20. Yorimitsu, T., Mimaki, A., Yakushi, T. & Homma, M. The conserved charged residues of the C-terminal region of FliG, a rotor component of the $Na^+$-driven flagellar motor. *J. Mol. Biol.* **334**, 567–583 (2003).
21. Yorimitsu, T., Sowa, Y., Ishijima, A., Yakushi, T. & Homma, M. The systematic substitutions around the conserved charged residues of the cytoplasmic loop of $Na^+$-driven flagellar motor component PomA. *J. Mol. Biol.* **320**, 403–413 (2002).
22. Welch, M., Oosawa, K., Aizawa, S. & Eisenbach, M. Phosphorylation-dependent binding of a signal molecule to the flagellar switch of bacteria. *Proc. Natl Acad. Sci. U.S.A.* **90**, 8787–8791 (1993).
23. Sarkar, M. K., Paul, K. & Blair, D. Chemotaxis signaling protein CheY binds to the rotor protein FliN to control the direction of flagellar rotation in *Escherichia coli*. *Proc. Natl Acad. Sci. U.S.A.* **107**, 9370–9375 (2010).
24. Zhao, R., Pathak, N., Jaffe, H., Reese, T. S. & Khan, S. FliN is a major structural protein of the C-ring in the *Salmonella typhimurium* flagellar basal body. *J. Mol. Biol.* **261**, 195–208 (1996).
25. Thomas, D. R., Francis, N. R., Xu, C. & DeRosier, D. J. The three-dimensional structure of the flagellar rotor from a clockwise-locked mutant of *Salmonella enterica* serovar Typhimurium. *J. Bacteriol.* **188**, 7039–7048 (2006).
26. Terashima, H., Fukuoka, H., Yakushi, T., Kojima, S. & Homma, M. The *Vibrio* motor proteins, MotX and MotY, are associated with the basal body of $Na^+$-driven flagella and required for stator formation. *Mol. Microbiol.* **62**, 1170–1180 (2006).
27. Hosogi, N., Shigematsu, H., Terashima, H., Homma, M. & Nagayama, K. Zernike phase contrast cryo-electron tomography of sodium-driven flagellar hook-basal bodies from *Vibrio alginolyticus*. *J. Struct. Biol.* **173**, 67–76 (2010).
28. Kojima, S., Shinohara, A., Terashima, H., Yakushi, T., Sakuma, M., Homma, M., Namba, K. & Imada, K. Insights into the stator assembly of the *Vibrio* flagellar motor from the crystal structure of MotY. *Proc. Natl Acad. Sci. U.S.A.* **105**, 7696–7701 (2008).
29. Okabe, M., Yakushi, T. & Homma, M. Interactions of MotX with MotY and with the PomA/PomB sodium ion channel complex of the *Vibrio alginolyticus* polar flagellum. *J. Biol. Chem.* **280**, 25659–25664 (2005).
30. Terashima, H., Koike, M., Kojima, S. & Homma, M. The flagellar basal body-associated protein FlgT is essential for a novel ring structure in the sodium-driven *Vibrio* motor. *J. Bacteriol.* **192**, 5609–5615 (2010).
31. Fukuoka, H., Wada, T., Kojima, S., Ishijima, A. & Homma, M. Sodium-dependent dynamic assembly of membrane complexes in sodium-driven flagellar motors. *Mol. Microbiol.* **71**, 825–835 (2009).
32. Fukuoka, H., Sowa, Y., Kojima, S., Ishijima, A. & Homma, M. Visualization of functional rotor proteins of the bacterial flagellar motor in the cell membrane. *J. Mol. Biol.* **367**, 692–701 (2007).
33. Li, H. & Sourjik, V. Assembly and stability of flagellar motor in *Escherichia coli*. *Mol. Microbiol.* **80**, 886–899 (2011).
34. Morimoto, Y. V., Nakamura, S., Kami-ike, N., Namba, K. & Minamino, T. Charged residues in the cytoplasmic loop of MotA are required for stator assembly into the bacterial flagellar motor. *Mol. Microbiol.* **78**, 1117–1129 (2010).
35. Kusumoto, A., Kamisaka, K., Yakushi, T., Terashima, H., Shinohara, A. & Homma, M. Regulation of polar flagellar number by the *flhF* and *flhG* genes in *Vibrio alginolyticus*. *J. Biochem.* **139**, 113–121 (2006).
36. Guzman, L. M., Belin, D., Carson, M. J. & Beckwith, J. Tight regulation, modulation, and high-level expression by vectors containing the arabinose PBAD promoter. *J. Bacteriol.* **177**, 4121–4130 (1995).
37. Yorimitsu, T., Sato, K., Asai, Y., Kawagishi, I. & Homma, M. Functional interaction between PomA and PomB, the $Na^+$-driven flagellar motor components of *Vibrio alginolyticus*. *J. Bacteriol*. **181**, 5103–5106 (1999).
38. Koike, M., Terashima, H., Kojima, S. & Homma, M. Isolation of basal bodies with C-ring components from the $Na^+$-driven flagellar motor of *Vibrio alginolyticus*. *J. Bacteriol*. **192**, 375–378 (2010).
39. Nishioka, N., Furuno, M., Kawagishi, I. & Homma, M. Flagellin-containing membrane vesicles excreted from *Vibrio alginolyticus* mutants lacking a polar-flagellar filament. *J. Biochem*. **123**, 1169–1173 (1998).
40. Yagasaki, J., Okabe, M., Kurebayashi, R., Yakushi, T. & Homma, M. Roles of the intramolecular disulfide bridge in MotX and MotY, the specific proteins for sodium-driven motors in *Vibrio* spp. *J. Bacteriol.* **188**, 5308–5314 (2006).
41. Kawagishi, I., Okunishi, I., Homma, M. & Imae, Y. Removal of the periplasmic DNase before electroporation enhances efficiency of transformation in a marine bacterium *Vibrio alginolyticus*. *Microbiology* **140**, 2355–2361 (1994).
42. Lee, L. K., Ginsburg, M. A., Crovace, C., Donohoe, M. & Stock, D. Structure of the torque ring of the flagellar motor and the molecular basis for rotational switching. *Nature* **466**, 996–1000 (2010).
43. Brown, P. N., Hill, C. P. & Blair, D. F. Crystal structure of the middle and C-terminal domains of the flagellar rotor protein FliG. *EMBO J.* **21**, 3225–3234 (2002).
44. Minamino, T., Imada, K., Kinoshita, M., Nakamura, S., Morimoto, Y. V. & Namba, K. Structural insight into the rotational switching mechanism of the bacterial flagellar motor. *PLoS Biol.* **9**, e1000616 (2011).
45. Suzuki, H., Yonekura, K. & Namba, K. Structure of the rotor of the bacterial flagellar motor revealed by electron cryomicroscopy and single-particle image analysis. *J. Mol. Biol.* **337**, 105–113 (2004).
46. Thomas, D. R., Morgan, D. G. & DeRosier, D. J. Rotational symmetry of the C ring and a mechanism for the flagellar rotary motor. *Proc. Natl Acad. Sci. U.S.A.* **96**, 10134–10139 (1999).
47. Young, H. S., Dang, H., Lai, Y., DeRosier, D. J. & Khan, S. Variable symmetry in *Salmonella typhimurium* flagellar motors. *Biophys. J*. **84**, 571–577 (2003).
48. Roberts, A. J., Numata, N., Walker, M. L., Kato, Y. S., Malkova, B., Kon, T., Ohkura, R., Arisaka, F., Knight, P. J., Sutoh, K. & Burgess, S. A. $AAA^+$ Ring and linker swing mechanism in the dynein motor. *Cell* **136**, 485–495 (2009).